From 1956 to 1958 he was Assistant Professor at the Technical University, Aachen. In 1958 he joined the U.S. Army Research and Development Laboratory in Fort Monmouth, NJ, where he performed basic research in free space and guided propagation of electromagnetic waves. From 1961 to 1964 he worked as a Member of the Research Staff of the Telefunken Company, Ulm, West Germany, on radar propagation studies and missile electronics. In 1964 he returned to the U.S. Army Electronics Command, Fort Monmouth, NJ, and has since been active in the fields of electromagnetic-wave propagation, diffraction and scatter theory, theoretical optics, and antenna theory. Recently, he has been involved, in particular, in millimeter-wave antenna and propagation studies.

Dr. Schwering is a Visiting Professor at Rutgers University. He is a member of URSI Commission B and of Sigma Xi, and was a recipient of the 1961 Best Paper Award of the IRE Professional Group on Antennas and Propagation (jointly with G. Goubau).

Song-Tsuen Peng (M'74–SM'82) was born in Taiwan, China, on February 19, 1937. He received the B.S. degree in electrical engineering from the National Cheng-Kung University, in 1959, the M.S. degree in electronics from the National Chiao-Tung University, in 1961, both in Taiwan, and the Ph.D. degree in electrophysics from the Polytechnic Institute of Brooklyn, Brooklyn, NY, in 1968.

Since 1968 he has been with the Polytechnic Institute of New York and is currently a Research Associate Professor in the Department of Electric Engineering and Computer Science. He has participated in many research programs in cooperation with government and industrial laboratories in the U.S. and also in academic exchanges with universities abroad. He has carried out research in the areas of wave propagation, radiation, diffraction, and nonlinear electromagnetics, and has published numerous papers in electromagnetics optics and acoustics.

Dr. Peng is a member of Sigma Xi.

Theory of Optically Controlled Millimeter-Wave Phase Shifters

AILEEN M. VAUCHER, CHARLES D. STRIFFLER, MEMBER, IEEE, AND CHI H. LEE, MEMBER, IEEE

Abstract—**In this paper we analyze the millimeter-wave propagation characteristics of a dielectric waveguide containing a plasma-dominated region. Such a device presents a new method for controlling millimeter-wave propagation in semiconductor waveguides via either optical or electronic means resulting in ultrafast switching and gating. We have calculated the phase shift and attenuation resulting from the presence of the plasma. Higher order modes, both TE and TM, as well as millimeter-wave frequency variation, are studied in both Si and GaAs dielectric waveguides. We have also formulated a surface plasma model that is a good approximation to the more elaborate volume plasma model. Phase shifts are predicted to be as high as 1400°/cm for modes operating near cutoff. These modes suffer very little attenuation when the plasma region contains a sufficiently high carrier density.**

I. Introduction

WE ARE CURRENTLY witnessing a resurgence of interest in millimeter-wave technology. The frequency band extending from 30 to 1000 GHz is attractive in several respects. Devices operating above *K*-band frequencies offer greater carrier bandwidth, better spatial resolution, and a more compact technology than presently used *X*- and *K*-band systems. Millimeter- and submillimeter-wave systems also have some advantages over optical systems, such as better atmospheric propagation in selected bands and a technology more amenable to frequency multiplexing [1]–[3], while retaining good angular resolution of the latter. A basic problem is how to effectively preserve these benefits. Our approach to the solution of this problem promises to yield much larger modulation bandwidths than are realizable with optical systems, while preserving the economy of the millimeter-wave system over a given carrier frequency band.

One of the important parts of the microwave and/or millimeter-wave system is the waveguide. At microwave frequencies, metal waveguides are commonly used. At higher frequencies, either microstrip or dielectric waveguide structures become more attractive. Microstrip transmission lines are used up to 30 GHz. For frequencies greater than 30 GHz, the losses in microstrip structures are high, and fabrication techniques become more difficult due to the small strip width and the substrate thickness. Dielectric rectangular waveguides become an alternative to the expensive metal waveguides. The use of high-purity semiconductor materials as dielectric waveguides is particularly important since active devices such as oscillators, Gunn or IMPATT diodes, mixers/detectors, and modulators can be fabricated monolithically with the semiconducting waveguides.

Manuscript received May 3, 1982; revised August 6, 1982. This work was supported in part by the Harry Diamond Laboratory; the U.S. Army; the Minta Martin Aeronautical Research Fund, College of Engineering, University of Maryland; and the University of Maryland Computer Science Facility.

The authors are with the Electrical Engineering Department, University of Maryland, College Park, MD 20742.

0018-9480/83/0200-0209$01.00 ©1983 IEEE

One important aspect of millimeter-wave devices is the control of the phase and amplitude of a wave propagating through the waveguide. The use of semiconductor bulk phenomena in implementing microwave control components has been discussed [4]. The principal phenomena explored have been the dielectric and conductive properties of the plasma state. A frequency-scanning millimeter-wave antenna utilizing periodic metallic-stripe perturbations on a silicon waveguide has been demonstrated [5]. Millimeter-wave dielectric image-guide integrated devices have been developed [6]. In the optical region, there are a variety of controllable waveguide devices which have not found their counterparts in the millimeter-wave region. High-speed light modulators that make use of the electrooptic, acoustooptic, and magnetooptic effects in bulk material have been described [7].

Phase shifting is a fundamental control operation. A general approach to this operation, used extensively at both optical [8] and microwave [9] frequencies, is to alter the phase velocity along a fixed interval of a guiding medium. In this case, the phase shift per unit length is equal to the change in the propagation constant of the guided wave. One well-known method of altering the dispersion of millimeter waves is to introduce a plasma into the guiding medium. In their work, Jacobs *et al.* [10] have demonstrated that the phase shift can be accomplished by injecting plasma with p-i-n diodes [11]. Similar work at low frequency has been demonstrated recently by Glance [12]. There are several shortcomings of p-i-n-diode-controlled millimeter-wave devices: a) large phase shifts have not been achieved due to excess heating of the waveguide; b) there are large losses (> 6dB) due to excess metallization for contact to the junction region; and c) the p-i-n diode becomes an integral part of the waveguide. This leads to complex boundary conditions and poor electrical isolation between the p-i-n diode and the waveguide structure.

Recently, we have demonstrated a way of circumventing the above difficulties. By illuminating the guide with above-bandgap radiation, we have created the basic element of a new class of device, an optically controlled millimeter-wave phase shifter and modulator. Optical control offers the following advantages: a) near perfect isolation; b) low static and dynamic insertion losses in some regimes; c) fast response; d) high power handling capability; e) when picosecond pulses are used, it is possible for extremely high density plasmas to be injected without damaging the material; f) by proper choice of semiconducting material and laser wavelength, one can generate plasma with any desirable density distributions and at any desirable time; g) ultrafast switching and gating of millimeter-wave signals is possible; and h) using picosecond exciting-probing techniques, the dynamic evolution of the injected plasma can be studied in detail. Parameters related to transport properties of the carriers can be accurately determined.

This paper analyzes in detail the changes that occur in the propagation characteristics of millimeter waves in a dielectric waveguide when a plasma-dominated region is present. The model and method analysis are presented in [13]. In that paper, both the experimental and theoretical studies concentrated primarily on the propagation of the dominant lowest order model (TM) denoted by $E^y_{1,1}$ for 94-GHz waves in a silicon waveguide. In practice, it has been found that for waves propagating in an over-sized waveguide with a plasma covered region, the waves will not remain in the fundamental mode. In this paper, we extend the analysis to include higher order TM modes $E^y_{p,q}$ and TE modes $E^x_{p,q}$. Calculations have also been carried out at frequencies other than 94 GHz. To understand the multimode propagation characteristics more fully, a model based on a surface plasma is devised, and the results compared with those obtained by a more elaborate calculation involving a finite thickness plasma layer. It is found that the surface plasma model gives a good approximation for plasma layers less than 10 μm in thickness. This is significant since we now have a simple theoretical model to predict the phase shift and to understand the mode-coupling mechanism in a general situation for plasma-controlled phase-shifting devices of arbitrary dimensions.

Recently, we have demonstrated the operation of a wide-bandwidth, high-repetition rate opto-electronic modulator for 94-GHz signals based on a plasma-controlled Cr-doped GaAs waveguide [14]. The rapid phase and amplitude modulation are achieved by using picosecond optical pulses to inject a plasma into the waveguide. In Cr-doped GaAs, in contrast to silicon, the electron-hole plasma recombines rapidly, i.e., in less than 100 ps, thus resulting in a high-speed, wide-bandwidth, and high-repetition rate operation of a millimeter-wave modulator. Therefore, in this paper, we extend our theoretical investigation of dielectric materials to include GaAs.

In Section II, the concept of a plasma-controlled dielectric waveguide is reviewed and earlier experimental results are summarized. The complete analysis, including the presentation of the surface plasma model, is then treated in Section III. It should be pointed out that the analysis presented here is quite general; it can be applied to the plasma-controlled dielectric waveguide devices no matter whether the plasma injection is by optical means, as in this work, or by electronic means, as in the work reported by Jacobs *et al.* [10].

II. Concept of Plasma-Controlled Dielectric Waveguide with Preliminary Experimental Results

Shown in Fig. 1 is a schematic of the optically controllable phase shifter. It consists of a rectangular semiconductor waveguide with tapered ends to allow efficient transition of millimeter waves both to and from a conventional metal waveguide. Optical control is realized when the broadwall of the semiconductor guide is illuminated by light generated by either a proximal source or one removed by a suitable optical guiding medium. The width a and height b of the guide are selected so that it supports an $E^y_{1,1}$ mode.

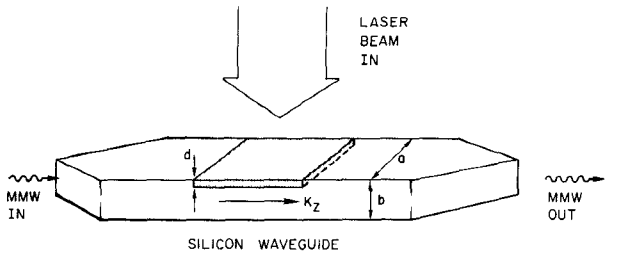

Fig. 1. Schematic diagram of the optically controlled phase shifter. The propagation vector in the guide is k_z, d is the depth of the injected plasma layer, a is the width of the guide, and b is the height of the guide.

The initial depth of plasma injection is controlled by selecting an appropriate combination of optical radiation wavelength and semiconductor absorption properties.

At sufficiently small injection depths, the final thickness of the plasma is determined primarily by processes of carrier diffusion and recombination. The effect of the plasma-occupied volume is to introduce a layer whose index of refraction at the millimeter-wave frequency is larger than that of the remaining volume of the waveguide. As the optical-illumination intensity increases from a low value, a significant phase shift will not appear until the plasma frequency exceeds the frequency of the guided millimeter wave, after which it will rapidly rise and eventually saturate. The form and magnitude of the phase shift versus the intensity of illumination, and hence the plasma density, depends in detail on the material and geometrical factors that characterize the optically perturbed guiding structure, and the determination of these quantities requires a detailed solution of the corresponding boundary value problems. The optically induced phase shift $\Delta\phi$ for a given section of waveguide of length l is determined by computing the propagation constant in the z direction; first, in the absence of the injected plasma k_z, and then with the plasma k_z'; thus, $\Delta\phi = (k_z' - k_z)l$.

Comparison between the experimental and the theoretical results presented in [13] and in Section III are shown in Fig. 2. The correspondence between the data and the theoretically predicted curve is excellent. As shown in Fig. 2, we observed a maximum phase shift of 59° at 94 GHz for a plasma column 1.6 mm in length with dynamic insertion loss of less than one decibel.

By slightly variations of the phase-shifting technique, we have also demonstrated opto-electronic switching and gating of millimeter-wave signals at 94 GHz by an optically induced plasma in a silicon waveguide [15]. A millimeter-wave pulse width as short as one nanosecond and variable to tens of nanoseconds can readily be obtained by this technique. We conclude from these studies that optical injection of plasma is superior to electrical injection because of its near-perfect isolation. The geometry and nature of the injected-plasma column are more amenable to analysis. Excellent agreement between experiment and theory encourages further study and a search for better experimental configurations to realize a new class of devices with high efficiency.

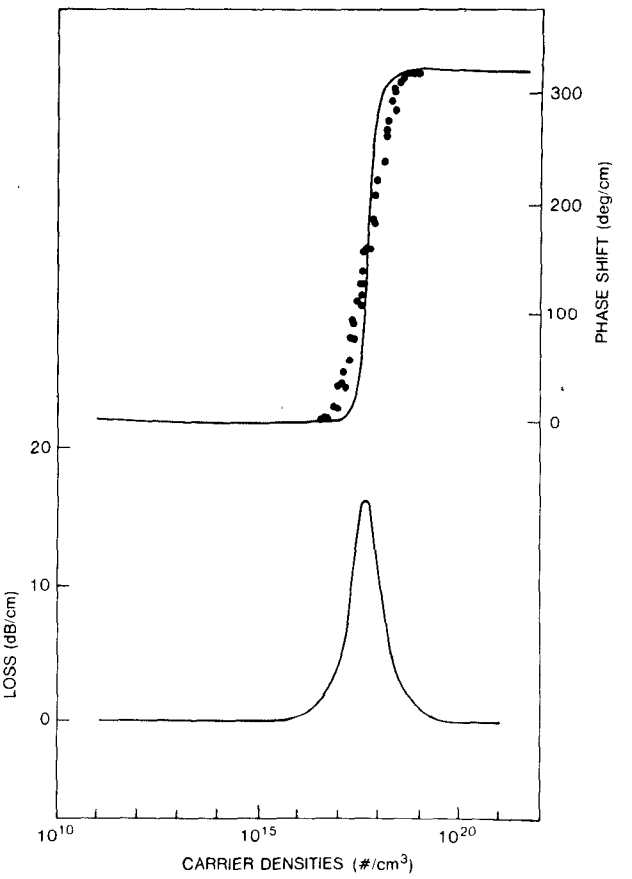

Fig. 2. Measured phase shift normalized to units of deg/cm [15].

III. Model and Analysis of a Plasma-Controlled Dielectric Waveguide

The geometry of the rectangular dielectric–plasma guide model is shown in Fig. 3. The guide cross section is in the $x-y$ plane, and the z coordinate represents the direction of propagation. The dimensions of the guide are denoted by a and b, and the plasma region thickness by t_p. The medium surrounding the waveguide is air. The relative dielectric constant and refractive index of the dielectric region $0 < y < b - t_p$ are ϵ_r and $n_r = \sqrt{\epsilon_r}$, respectively, and those of the dielectric–plasma region $b - t_p < y < b$ are [13]

$$\epsilon_p = n_p^2 = \epsilon_r - \alpha \frac{\omega_{p\alpha}^2}{\omega^2 + \nu_\alpha^2} - j\alpha \frac{\omega_{p\alpha}^2}{\omega^2 + \nu_\alpha^2} \frac{\nu_\alpha}{\omega} \equiv (\eta - j\kappa)^2. \quad (1)$$

The free-charge contribution (plasma) is characterized by a plasma frequency $\omega_{p\alpha} = (q_\alpha^2 N_\alpha / m_\alpha \epsilon_0)^{1/2}$ of each species of density N_α, and an effective collision frequency ν_α. These various species in an optically formed plasma are denoted by thermally ionized and photo-induced holes (light and heavy) and electrons. The values of the various species properties, that is, density, effective mass, and collision frequency, are listed in Fig. 4(a) for Si and Fig. 4(b) for GaAs. In Fig. 4(a) the real part η and imaginary part κ of the refractive index for Si (see (1)) are plotted as a function

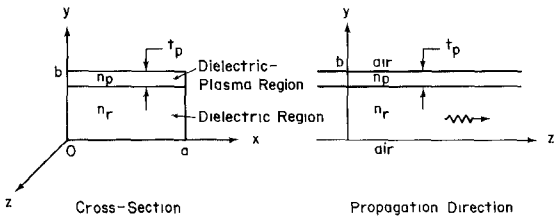

Fig. 3. Geometry of dielectric–plasma waveguide model.

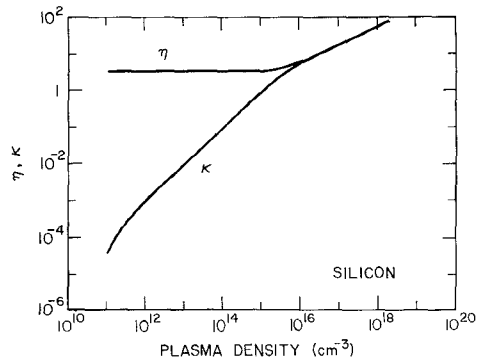

(a)

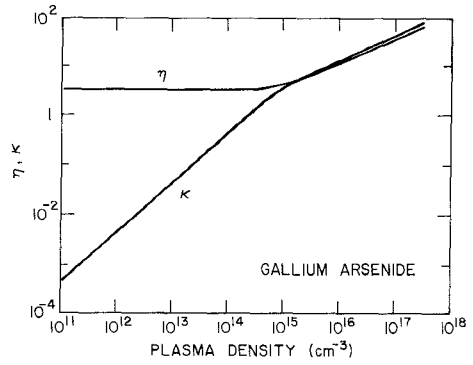

(b)

Fig. 4. (a) Plot of the plasma region refractive index versus plasma density in Si at 94 GHz. Here $P_L = 0.14\ N_p$; $P_H = 0.86\ N_p$; $m_e^* = 0.259\ m_0$; $m_p^* = 0.38\ m_0$; $m_{P_L}^* = 0.16\ m_0$; $m_{P_H}^* = 0.49\ m_0$; $\mu_e = 1500\ \text{cm}^2/\text{V}\cdot\text{s}$; $\tau_e = 2.2\times10^{-13}$ s; $\mu_h = 600\ \text{cm}^2/\text{V}\cdot\text{s}$; $\tau_p = 1.3\times10^{-13}$ s; and $N_{p0} = 10^{11}\ \text{cm}^{-3}$ [16], [17]. (b) Plot of the plasma-region refractive index versus plasma density in GaAs at 94 GHz. Here $P_L = 0$, $P_H = N_p$; $m_e^* = 0.06\ m_0$; $m_p^* = 0.5\ m_0$; $m_{P_H} = 0.8\ m_0$; $\mu_e = 8800\ \text{cm}^2/\text{V}\cdot\text{s}$; $\tau_e = 3.3\times10^{-13}$ s; $\mu_h = 450\ \text{cm}^2/\text{V}\cdot\text{s}$; $\tau_p = 1.28\times10^{-13}$ s; and $N_{p0} = 1.4\times10^6\ \text{cm}^{-3}$ [18–20].

of plasma density for a 94-GHz wave. Likewise, in Fig. 4(b) the refractive index in the plasma–dielectric region for GaAs is plotted. For each material, note the metallic nature of the plasma region for plasma density above about $10^{16}\ \text{cm}^{-3}$ for Si and $10^{15}\ \text{cm}^{-3}$ for GaAs.

For the case of well-guided modes, the analysis is considerably simplified in that the dispersion equation is essentially decoupled between the x and y directions [21]. That is, if the fields in the dielectric are assumed to vary as $\exp i(\omega t - k_x x - k_y y - k_z z)$, we find that boundary conditions in x determine k_x, those in y determine k_y, and from these one can then determine k_z. With these assumptions, the modes decouple into TM, called $E_{p,q}^y$, and TE, called $E_{p,q}^x$ modes. The propagation constant k_z is computed for the cases with and without the presence of the plasma region, k_z' (complex), k_z (real), respectively, and from these the plasma induced phase shift $\Delta\phi$ for a given length of waveguide l can be computed by

$$\Delta\phi = (\text{Re}\,k_z' - k_z)l, \text{ rad} \tag{2}$$

and the attenuation coefficient by

$$\alpha = \text{Im}\,k_z', \text{ cm}^{-1}. \tag{3}$$

Specifically, in a waveguide of dimensions a and b and with *no plasma present*, $n_p = n_r(\omega_{p\alpha} = 0)$, k_x and k_y for the $E_{p,q}^y$ mode are approximated by [21]

$$k_{x_{\text{TM}}} \simeq \frac{p\pi}{a}\left[1 + \frac{1}{\pi a}\frac{\lambda_0}{(\epsilon_r - 1)^{1/2}}\right]^{-1} \tag{4}$$

and

$$k_{y_{\text{TM}}} \simeq \frac{q\pi}{b}\left[1 + \frac{1}{\pi\epsilon_r b}\right]\frac{\lambda_0}{(\epsilon_r - 1)^{1/2}}^{-1}. \tag{5}$$

Here p is the number of extrema in the x direction, q is the number of extrema in the y direction, and λ_0 is the free-space wavelength of the propagating wave. Similarly, for well-guided $E_{p,q}^x$ modes, k_x and k_y are approximated by [21]

$$k_{x_{\text{TE}}} \simeq \frac{p\pi}{a}\left[1 + \frac{1}{\pi\epsilon_r a}\frac{\lambda_0}{(\epsilon_r - 1)^{1/2}}\right]^{-1} \tag{6}$$

and

$$k_{y_{\text{TE}}} \simeq \frac{q\pi}{b}\left[1 + \frac{1}{\pi b}\frac{\lambda_0}{(\epsilon_r - 1)^{1/2}}\right]^{-1}. \tag{7}$$

With these values of k_x and k_y, we can compute k_z in the guide without the plasma present

$$k_z = \left(n_r^2\frac{\omega^2}{c^2} - k_x^2 - k_y^2\right)^{1/2} \tag{8}$$

where k_x and k_y are given by either their TM values (4) and (5), or their TE values (6) and (7).

Now consider the case when the *plasma layer is present*, as shown in Fig. 3. Again, assuming the decoupling due to well-guided modes is valid, we note that the solutions for k_x for the $E_{p,q}^y$ and $E_{p,q}^x$ modes are given by (4) and (6). In the y direction, the solution for k_y for TM($E_{p,q}^y$) waves is found by solving [13]

$$\tan^{-1}\frac{K_a\epsilon_r}{k_r} + \tan^{-1}\left\{\frac{k_p}{k_r}\frac{\epsilon_r}{\epsilon_p}\tan\left[\tan^{-1}\left(\frac{K_a\epsilon_p}{k_p}\right) - k_p t_p\right]\right\} - k_r(b - t_p) + (q-1)\pi = 0 \tag{9}$$

and for TE($E_{p,q}^x$) waves

$$\tan^{-1}\frac{K_a}{k_r} + \tan^{-1}\left\{\frac{k_p}{k_r}\tan\left[\tan^{-1}\left(\frac{K_a}{k_p}\right) - k_p t_p\right]\right\} - k_r(b - t_p) + (q-1)\pi = 0. \tag{10}$$

In (9) and (10), we have defined the various k_y's in each

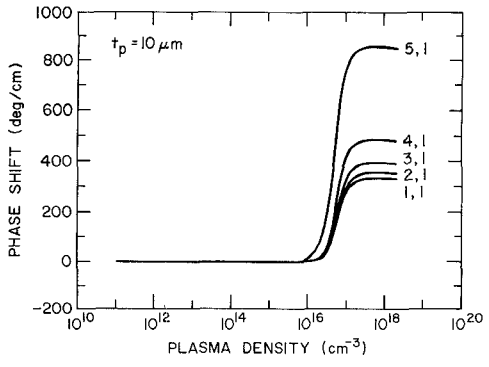

(a)

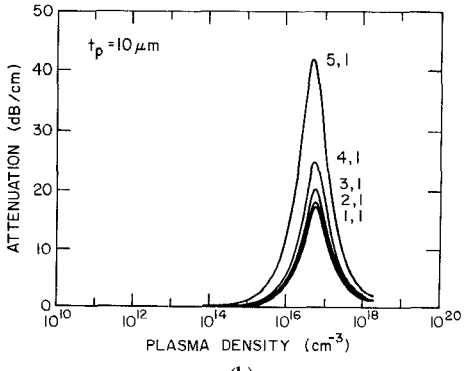

(b)

Fig. 5. (a) Phase-shift properties in a 2.4×1-mm^2 Si waveguide at 94 GHz with respect to plasma density for a plasma region thickness of 10 μm. Parametric dependence is the TM mode $E^y_{p,q}$. (b) Attenuation properties in a 2.4×1-mm^2 Si waveguide at 94 GHz with respect to plasma density for plasma region thickness of 10 μm. Parametric dependence is the TM mode $E^y_{p,q}$.

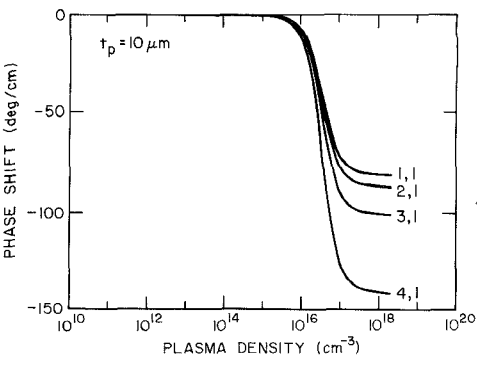

(a)

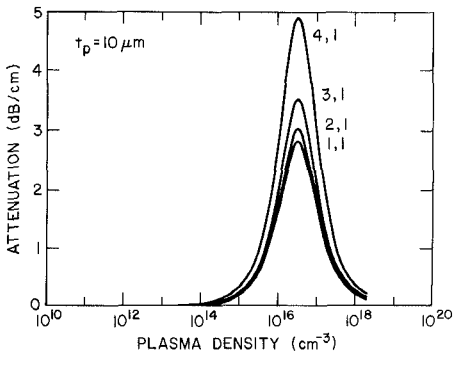

(b)

Fig. 6. (a) Phase shift properties in a 2.4×1-mm^2 Si waveguide at 94 GHz with respect to plasma density for a plasma region thickness of 10 μm. Parametric dependence is the TE mode $E^x_{p,q}$. (b) Attenuation properties in a 2.4×1-mm^2 Si waveguide at 94 GHz with respect to plasma density for a plasma region thickness of 10 μm Parametric dependence is the TE mode $E^x_{p,q}$.

region (Fig. 3) as

$$K_a = \frac{2\pi}{\lambda_0}\left(n_\omega^2 - 1\right)^{1/2}$$

$$k_r = \frac{2\pi}{\lambda_0}\left(n_r^2 - n_\omega^2\right)^{1/2}$$

$$k_p = \frac{2\pi}{\lambda_0}\left(n_p^2 - n_\omega^2\right)^{1/2} \qquad (11)$$

and n_ω is the effective refractive index of the wave in the decoupled guide. In the plasma layer, the index n_p is complex and depends upon the density of the plasma (see (1)). Substituting the k_y's into (9) and (10) results in transcendental equations for n_ω. These equations are solved numerically for n_ω, from which k_r is determined. The value of k_r is the value of k_y in the dielectric region in the presence of the plasma layer and thus k_z' may be found by

$$k_z' = \left(n_r^2\frac{\omega^2}{c^2} - k_x^2 - k_r^2\right)^{1/2}. \qquad (12)$$

We can then compute the phase shift $\Delta\phi$ and attenuation α from (2) and (3), using (8) and (12).

In [15], plots of phase shift and attenuation versus plasma density, with plasma region thickness a parameter, were shown for the lowest order E^y mode, i.e., $E^y_{1,1}$. The Si waveguide cross sections for those plots were 2.4×1 mm^2 and 1×0.5 mm^2, and the plasma thickness was varied from 1 μm to half the guide depth. In this paper, we have calculated $\Delta\phi$ and α as a function of the plasma density for a rectangular Si waveguide of dimensions 2.4×1 mm^2 for all $E^y_{p,q}$ and $E^x_{p,q}$ modes that can propagate for a plasma region thickness of 10 μm. The results of the calculations are shown in Figs. 5 and 6. In Fig. 5(a) the phase shift per centimeter is plotted as a function of the plasma density for the $E^y_{1,1}$ through the $E^y_{5,1}$ modes, which are the only $E^y_{p,1}$ modes that can propagate in this guide. The corresponding loss in dB/cm is plotted in Fig. 5(b). As the plasma density increases from 10^{15} cm^{-3} to 10^{20} cm^{-3}, the skin depth in Si decreases from more than 200 μm to less than 1 μm. When the skin depth is equal to or larger than the plasma layer thickness, the millimeter wave penetrates deeply into the plasma layer causing loss. The maximum loss occurs when the skin depth is about equal to the layer thickness. The higher order modes have more loss in this regime than the lower order modes, because more of the wave power is concentrated in the plasma region when a higher order mode is propagating in the guide. As the plasma density increases further, the skin depth decreases. When the skin depth is less than the thickness of the plasma layer, the plasma region begins to act as a metallic conductor and the dielectric waveguide becomes an image line. The attenuation then drops off rapidly with increasing plasma density. The maximum phase shift of the higher order modes is also larger than that of the lower order modes because the

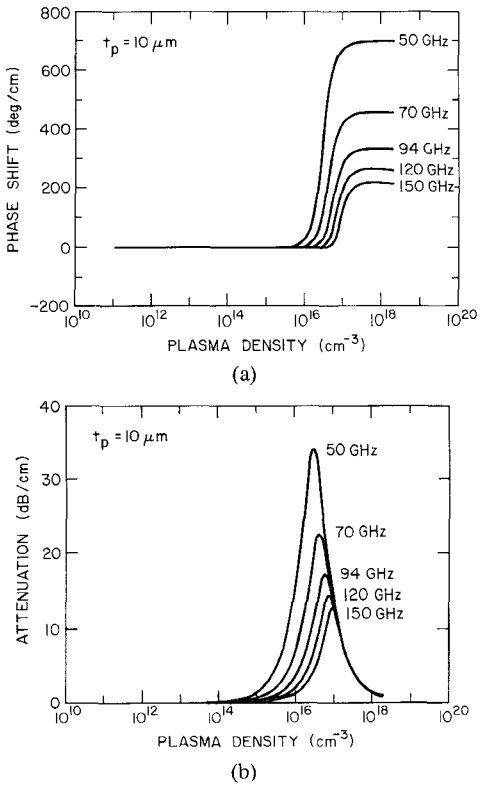

Fig. 7 (a) Phase-shift properties in a 2.4×1-mm² Si waveguide with respect to plasma density for a plasma-region thickness of 10 μm and the lowest order TM mode $E^y_{1,1}$. Parametric dependence is the frequency of the millimeter wave. (b) Attenuation properties in a 2.4×1-mm² Si waveguide with respect to plasma density for a plasma-region thickness of 10 μm and the lowest order TM mode $E^y_{1,1}$. Parametric dependence is the frequency of the millimeter wave.

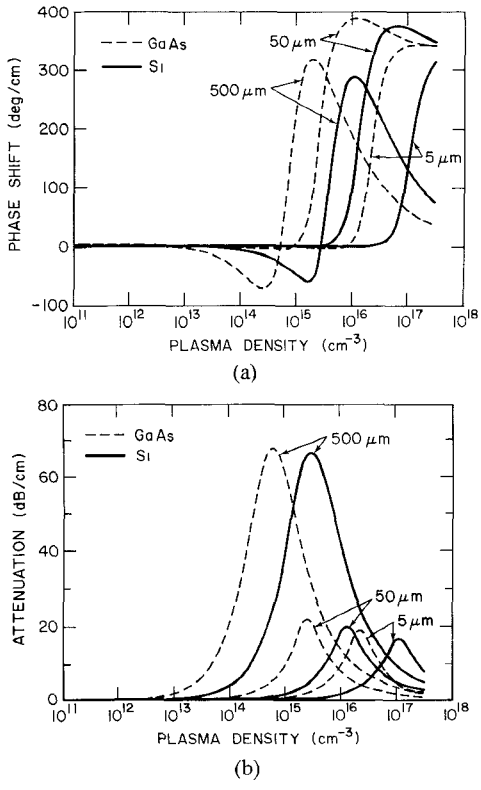

Fig. 8. (a) Comparison of the phase-shift characteristics of an $E^y_{1,1}$ mode propagating at 94 GHz in a 2.4×1-mm² waveguide for Si (solid lines) and GaAs (dashed lines) plotted with respect to plasma density. The three sets of curves correspond to plasma depths of 500 μm, 50 μm, and 5 μm, respectively. (b) Comparison of the attenuation characteristics of an $E^y_{1,1}$ mode propagating at 94 GHz in a 2.4×1-mm² waveguide for Si (solid lines) and GaAs (dashed lines) plotted with respect to plasma density The three sets of curves correspond to plasma depths of 500 μm, and 50 μm, and 5 μm, respectively.

waveguide becomes more dispersive closer to cutoff. The other two TM modes this guide is capable of supporting at 94 GHz are the $E^y_{1,2}$ and $E^y_{2,2}$ modes, both of which are of higher order than the $E^y_{1,1}$ mode. Their maximum phase shifts are 1000°/cm and 1450°/cm, respectively.

Plots of the phase shift and attenuation curves for the TE modes, $E^x_{1,1}$ through $E^x_{4,1}$, in the 2.4×1-mm² guide at 94 GHz are shown in Fig. 6(a) and (b) for the 10-μm plasma layer. The results are similar to those found previously for the $E^y_{p,q}$ modes, except that the magnitude of the maximum phase shift is less and the maximum loss in the guide is less, reflecting the different field distribution requirements between the TE and TM modes.

The effect of varying the frequency of the millimeter wave in the 2.4×1-mm² guide for a 10-μm plasma depth is to shift the attenuation peak and the onset of the phase shift. This is shown in Fig. 7(a) and (b) for the $E^y_{1,1}$ wave. This is to be expected since the skin depth is a decreasing function of frequency; therefore, the plasma density at which the greatest amount of interaction between the plasma and the wave occurs increases as frequency is increased. Also, as the frequency is lowered, the maximum phase shifts and attenuations are larger. This is because the guide operates closer to cutoff at the lower frequencies. For a frequency of 50 GHz, only the mode shown, $E^y_{1,1}$, can propagate in the waveguide.

In Fig. 8(a) and (b), we have plotted the results for a 2.4×1-mm² GaAs waveguide. Because the features with respect to multimode and frequency variation are similar to those presented for Si, we have displayed only the lowest order TM mode $E^y_{1,1}$ results at 94 GHz with plasma thickness a parameter. For comparison, the Si guide results are displayed as solid curves. The general features of the GaAs curves are the same as those for Si; however, the curves are shifted toward lower plasma densities consistent with the shift in the dielectric properties of GaAs versus Si shown in Fig. 4.

A. Surface Model of the Plasma

A means of simplifying the calculation of the propagation constant k_x in the presence of the plasma is to assume that the plasma is located only at the surface with a surface plasma density

$$N_{s\alpha} = N_\alpha t_p, \text{ cm}^{-2} \tag{13}$$

where N_α is the volume density of each species α, and t_p is the thickness of the plasma. With this simplification, the plasma effect only appears in the boundary condition at $y = b$. A picture of this simplified model is shown in Fig. 9. The analysis proceeds as before by assuming that the solutions for k_x and k_y are decoupled. Again we find k_x is given by (4) and (6). We examine the plasma's reaction to

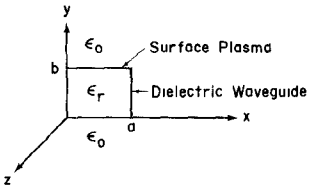

Fig. 9. Cross section of the plasma controlled dielectric waveguide with the plasma treated as a surface density.

the EM fields in terms of the linearized charge density ρ and a linearized current density $\vec{J}$, where

$$\rho = \sum_\alpha q_\alpha n_\alpha$$

$$\vec{J} = \sum_\alpha q_\alpha N_\alpha \vec{v}_\alpha. \tag{14}$$

Please note that N_α is the zeroth-order density of species α, and n_α represents the linearized response to the millimeter wave. Likewise, since the zeroth-order velocity of each species α is zero, $\vec{v}_\alpha$ represents the linearized velocity response to the millimeter wave. We use the integral form of Maxwell's Equations to find the boundary condition at $y = b$. The plasma quantities n_α and $\vec{v}_\alpha$ are found from the linearized fluid equations to be

$$n_\alpha = \frac{q_\alpha}{m_\alpha \omega} \frac{1}{\omega - i\nu_\alpha} \left\{ n_{\alpha 0} \left[\frac{\partial E_x}{\partial x} + \frac{\partial E_y}{\partial y} - ik_z E_z \right] + E_y \frac{\partial n_{\alpha 0}}{\partial y} \right\} \tag{15}$$

and

$$\vec{v}_\alpha = \frac{-iq_\alpha}{m_\alpha} \frac{\vec{E}}{\omega - i\nu_\alpha}. \tag{16}$$

We have defined $n_{\alpha 0} = N_{s\alpha}\delta(y - b)$, that is, a plasma located only at the surface $y = b$.

For TM waves, the surface plasma acts as a surface current and the transcendental equation for k_r becomes

$$\tan^{-1}\epsilon_r \frac{K_a}{k_r} + \tan^{-1}\left\{ \epsilon_r \frac{K_a}{k_r} \left[\frac{1}{1 - K_a t_p (\epsilon_p - \epsilon_r)} \right] \right\} - k_r b + (q-1)\pi = 0 \tag{17}$$

where K_a and k_r are as in (11). For TE waves, the surface plasma acts as a surface charge and the transcendental equation for k_r becomes

$$\tan^{-1}\frac{K_a}{k_r} + \tan^{-1}\left\{ \frac{K_a}{k_r} \left[1 + \left(\frac{2\pi}{\lambda_0} \right)^2 \frac{t_p}{K_a} (\epsilon_p - \epsilon_r) \right] \right\} - k_r b + (q-1)\pi = 0. \tag{18}$$

While (17) and (18) are still transcendental, their solutions are much simpler than those of (9) and (10). Fig. 10(a) and (b) shows the results of the surface plasma model analysis in comparison to the volume model presented in the previous figures. Good agreement of the phase shifts and attenuations of the two models with respect to plasma density at small plasma depth for a TM wave at 94 GHz is seen. As the thickness of the plasma layer gets larger, the agreement becomes poorer, as expected. Similar agreement is found for the TE waves and for higher order modes of both the TE and TM waves. Clearly, the simplicity of this model will aid us in figure analysis pertaining to mode conversion of a single incident wave.

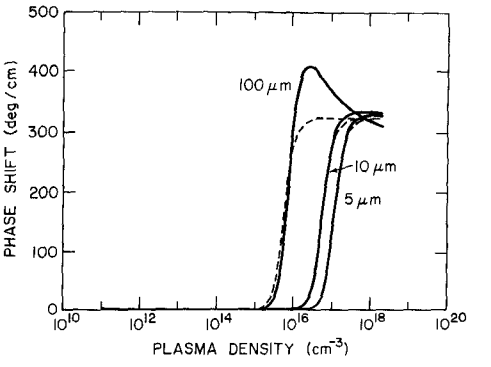

(a)

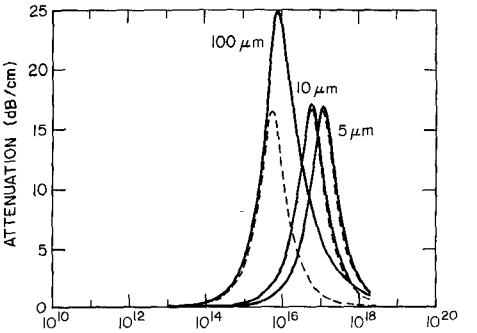

(b)

Fig. 10. (a) Comparison of the phase-shift characteristics of an $E^y_{1,1}$ mode propagating at 94 GHz in a 2.4 × 1-mm² Si waveguide for the surface model (dashed lines) and the volume model (solid lines) plotted with respect to plasma density. The three sets of curves correspond to plasma depths of 100 μm, 10 μm, and 5μm, respectively. (b) Comparison of the attenuation characteristics of an $E^y_{1,1}$ mode propagating at 94 GHz in a 2.4 × 1-mm² Si waveguide for the surface model (dashed lines) and the volume model (solid lines) plotted with respect to plasma density. The three sets of curves correspond to plasma depths of 100 μm, 10 μm, and 5 μm, respectively.

IV. Conclusion

We have analyzed in detail the steady-state millimeter-wave propagation characteristics of Si and GaAs dielectric waveguides that contain a plasma-dominated region. We have calculated the phase shift and attenuation properties resulting from the presence of the plasma. Higher order modes were examined as well as frequency variation of the millimeter wave for all modes capable of propagating in a given sized guide. A surface plasma model was formulated that greatly simplified the analysis, yet gave good agreement with the more elaborate volume model. This model will facilitate the computation of a more complicated situation where mode coupling effects may be important. Phase shifts as high as 1400°/cm are predicted for modes near cutoff. This analysis indicates that in an oversized guide where many modes can be present, the properties of all modes are similar in both their expected phase shift as well as their attenuation properties.

REFERENCES

[1] W. J. Tomlinson, "Wavelength multiplexing in multimode optical fibers," *Appl. Opt.*, vol. 16, pp. 2180–2194, 1977.

[2] M. Kobayashi and H. Herui, "Optical demultiplexer using coupling between nonidentical waveguides," *Appl. Opt.*, vol. 17, pp. 3253–3258, 1978.

[3] J. Minowa, K. Aoyama, and Y. Fujii, "Silicon blazed-grating for low loss optical multiplexer," in *Dig. Tech. Papers, 1979 IEEE/OSA Conf. on Laser Engineering and Applications*, paper 8.10, pp. 54–55.

[4] K. E. Mortenson, A. L. Armstrong, J. M. Borrego, and J. F. White, "A review of bulk semiconductor microwave control components," *Proc. IEEE*, vol. 59, pp. 1191–1200, 1971.

[5] K. L. Klohn, R. E. Horn, H. Jacobs, and E. Friedbergs, "Silicon waveguide frequency scanning linear array antenna," *IEEE Trans. Microwave Theory Tech.*, vol. MTT-26, pp. 764–773, 1978.

[6] J. A. Paul and Y. W. Chang, "Millimeter-wave image-guide integrated passive devices," *IEEE Trans. Microwave Theory Tech.*, vol. MTT-26, pp.751–754, 1978.

[7] I. P. Kaminow, "Optical waveguide modulators," *IEEE Trans. Microwave Theory Tech.*, vol. MTT-23, pp. 57–70, 1975.

[8] I. P. Kaminow, J. R. Carruthers, E. H. Turner, and L. W. Stulz, "Thin-film $LiNbO_3$ electro-optic light modulator," *Appl. Phys. Lett.*, vol. 22, pp. 540–542, 1973.

[9] R. V. Garver, *Microwave Diode Control Devices*. Dedham, MA: Artech House, 1976, ch. 10.

[10] H. Jacobs and M. M. Chrepta, "Electronic phase shifter for millimeter-wave semiconductor dielectric integrated circuits," *IEEE Trans. Microwave Theory Tech.*, vol. MTT-22, pp. 411–417, 1974.

[11] B. J. Levin and G. G. Wiedner, "Millimeter-wave phase shifters," *RCA Rev.*, vol. 34, pp. 489–505, 1973.

[12] B. Glance, "A fast low loss microstrip p-i-n phase shifter," *IEEE Trans. Microwave Theory Tech.*, vol. MTT-27, pp. 14–16, 1979.

[13] Chi H. Lee, Paul S. Mak, and A. P. DeFonzo, "Optical control of millimeter-wave propagation in dielectric waveguides," *IEEE J. Quantum Electron.*, vol. QE-16, pp. 277–288, 1980.

[14] M. G. Li, W. L. Cao, V. K. Mathur, and C. H. Lee, "Wide bandwidth high-repetition rate optoelectronic modulation of millimeter waves in GaAs waveguide," *Electron. Lett.*, vol. 14, pp. 454–456, 1982.

[15] Chi H. Lee, Paul S. Mak, and A. P. DeFonzo, "Millimeter-wave switching by optically generated plasma in silicon," *Electron. Lett.*, vol. 14, pp. 733–734, 1978.

[16] R. A. Smith, *Semiconductors*. Cambridge, MA: Cambridge, 1968, pp. 100 and 347.

[17] B. Lax and J. G. Mavorides, "Statistics and galvano-magnetic effects in germanium and silicon with warped energy surfaces," *Phys. Rev.*, vol. 100, pp. 1650–1657, 1955.

[18] *The Merck Index*, M. Windholz, Ed., 9th ed. Rahway, NJ: Merck, p. 561, 1976.

[19] *CRC Handbook of Chemistry and Physics*, R. C. Weast, Ed., 49th ed. Cleveland, OH: Chemical Rubber Company, 1968–1969, pp. E98–E102.

[20] C. O. Thurmond, "The standard thermodynamic function of the formation of electrons and holes in Ge, Si, GaAs, and GaP," *J. Electrochem. Soc.*, vol. 122, p. 1133, 1975.

[21] E. A. J. Marcatili, "Dielectric rectangular waveguide and direction coupler for integrated optics," *Bell Syst. Tech. J.*, vol. 48, p. 2103, 1969.

Charles D. Striffler (M'77) received the B.S. degree in science engineering and the M.S. and Ph.D. degrees in nuclear engineering at the University of Michigan in 1961, 1963, and 1972, respectively.

He was at Knolls Atomic Power Laboratory from 1965 to 1967, the Naval Research Laboratory from 1972 to 1975, and the University of Maryland since 1974, where he is an Associate Professor in Electrical Engineering. His areas of research in the plasma physics field are high-power microwave generation from rotating *E*-layers, collective ion acceleration using intense *E*-beams, and plasma millimeter-wave interactions in dielectric waveguides.

Aileen M. Vaucher was born in St. Paul, MN, in 1956. She received the B.S. degree in electrical engineering from the University of Minnesota, in 1979, and the M.S. degree from the University of Maryland, College Park, in 1980. She is currently working towards the Ph.D. degree in the field of electrophysics at the University of Maryland.

Her research interests are bulk GaAs lasers and plasma millimeter-wave interactions in dielectric waveguides.

Chi H. Lee (M'79) received the B.S. degree in electrical engineering from the National Taiwan University, Taipei, Taiwan, and the M.S. and Ph.D. degrees in applied physics from Harvard University, Cambridge, MA, in 1959, 1962, and 1968, respectively.

He was with the IBM San Jose Research Laboratory from 1967 to 1968. Since 1968 he has been with the University of Maryland, College Park, where he is now a Professor of Electrical Engineering. His areas of research include picosecond phenomena, nonlinear optical effects, and millimeter-wave devices.

Dr. Lee is a member of Sigma Xi and the American Physical Society.